Earthquake Geotechnical Engineering for Protection and Development of Environment and Constructions – Silvestri & Moraci (Eds)
© 2019 Associazione Geotecnica Italiana, Rome, Italy, ISBN 978-0-367-14328-2

Theoretical framework for the seismic design of anchored steel sheet pile walls

V.G. Caputo & R. Conti
Università di Roma Niccolò Cusano, Rome, Italy

G.M.B. Viggiani
University of Cambridge, Cambridge, UK

C. Prüm
ArcelorMittal - Global Research&Development, Esch-sur-Alzette, Luxembourg

ABSTRACT: Anchored Steel Sheet Pile (ASSP) walls are widely used as retaining structures in wharves and quays as an alternative to gravity concrete walls due to their ease of installation. Their seismic design is based on conventional pseudo-static approaches, often leading to uneconomic solution in high seismic areas. This paper addresses the dynamic behaviour of ASSP walls retaining dry cohesionless backfills, in order to investigate the possible failure mechanisms of the soil-wall system and the resulting permanent displacements. Simple limit equilibrium methods are developed to predict the internal forces in the structural members and to compute the critical acceleration of the soil-wall system, corresponding to which the strength of the soil is completely mobilised. Theoretical predictions are compared with the results of an extensive numerical study, including both pseudo-static and dynamic analyses. The key role of the critical acceleration for the structural and the geotechnical design of ASSP walls is highlighted, controlling both the maximum internal forces and the magnitude and trend of displacements.

1 INTRODUCTION

The prediction of the seismic response of anchored steel sheet pile (ASSP) walls is a complex issue, due to the great variety of factors and elements involved. The seismic earth pressure results from the dynamic loads induced by the earthquake motion, which is characterised by an intrinsic variability, and the non-linear soil behaviour. Particularly at port structures, shallow passive anchorages, in the form of continuous sheet pile, are usually preferred to concrete walls and to grouted anchors, due to their convenience in implementation. However, the need to deal with the passive resistance of the soil makes it more complicated to estimate the stiffness of the support provided by the anchor system, *e.g.* with respect to propped walls.

Conventional seismic design codes and standards usually comply with a force balanced pseudo-static approach, in which the effects of the earthquake motion are represented by an equivalent seismic coefficient $k_{h,eq}$, proportional to the expected *PGA* at ground surface. The assessment of the safety of the wall is based on triangular earth pressure distributions, determined using Mononobe-Okabe (MO) analysis (Mononobe & Matsuo, 1929; Okabe, 1926) on the active side and other methods involving log-spiral failure surfaces on the passive side (Anderson *et al.*, 2008). Though this approach is the basis for the design in many seismically active regions around the world, some issues are still being debated in the technical literature, of which perhaps the most important is the selection of an appropriate value for the equivalent seismic coefficient. After the seminal work by Richard & Elms (1979), the idea that the design acceleration may be reduced to take into account the ability of a retaining structure to accumulate permanent displacements in a ductile manner has already been accepted in the engineering practice. For instance, for yielding gravity walls, many empirical correlations have been

derived from the application of Newmark's sliding block procedure (Newmark, 1965), to estimate the permanent displacement of the wall, as a function of the ratio of the critical acceleration k_c, corresponding to which the strength of the system is completely mobilised and the wall starts to slide, to the *PGA*, when this is larger than unity. Well documented case histories indicate that a similar concept may be applied also to the performance based seismic design of ASSP walls, *i.e.* that a reduction of the maximum design acceleration paid by some amount of lateral permanent displacements may be acceptable. In the case of ASSP walls, however, wall-soil interaction is much more complex than for gravity retaining structures. The stiffness of the wall-anchor system needs to be investigated before reducing the *PGA* to account for possible displacements. Differently from other types of retaining structures, an outward translation of the wall would be rather improbable as a failure mechanism and also inconsistent with the aforementioned conventional design approach; moreover, several studies have demonstrated that a Newmark's calculation always under predicts the actual displacement of the wall whenever the assumptions inherent in the sliding block analysis are not fulfilled (Neelakantan *et.al*, 1990; Lai, 1998; Conti & Caputo, 2018).

As a further limitation of the conventional design procedure, the assumed earth pressure distribution implicitly requires failure of the foundation soil in front of the embedded length of the wall. A more rational approach to the design should contemplate all the possible ductile failure mechanisms under seismic conditions, both local and global ones, and design should be informed by a convenient choice of the preferred failure mechanism. A compromise between problem complexity, design procedure simplicity and reliability of the results may be found adopting simplified displacement methods. In this approach, the permanent displacements of the system are computed by integrating twice the acceleration time history exceeding a threshold critical acceleration $a_c = k_c g$ and the structural elements are designed to sustain the stresses corresponding to the critical acceleration.

2 LIMIT EQUILIBRIUM SOLUTIONS

2.1 *Retaining wall*

Figure 1 shows a wall retaining a dry cohesionless soil (unit weight γ, friction angle ϕ', friction angle at soil-wall interface δ) with horizontal ground surface. Retained height h, embedment depth D, and anchor location b are given. The same figure shows the proposed net earth pressure distribution on the retaining wall for a given pseudo-static coefficient k_h; this is derived assuming a quasi-rigid rotation of the wall around a pivot point in the embedded portion. It is

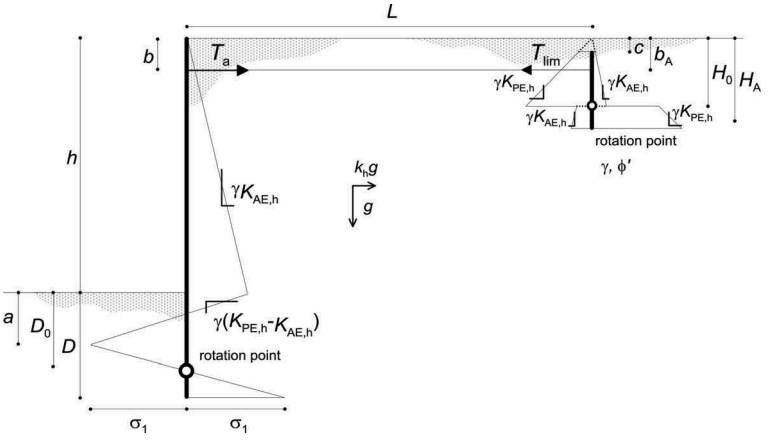

Figure 1. Typical layout of ASSP walls and proposed earth pressures distribution on the retaining wall and on the anchor wall.

assumed that, down to depth a below dredge level the horizontal displacements of the wall are large enough to attain active and passive limit states behind and in front of the wall, respectively, and, therefore, the net pressure distribution increases linearly with gradient γ ($K_{PE,h}$-$K_{AE,h}$), where the earth pressure coefficients, K_{PE} and K_{AE}, are computed using the solutions by Lancellotta (2007) and MO respectively. At larger depths, it is assumed that the net pressure starts to decrease, still linearly, changing sign at depth D_0, corresponding to the pivot point. At the toe of the wall, the net pressure will depend on a number of factors which are very difficult to evaluate and include, *e.g.*, the intensity of the seismic action, the flexibility of the wall and the restrain offered by the foundation soil at the toe; as a simplification, it is assumed to be the same as at depth a. Hence, the proposed diagram is completely defined once the depth, a, and the anchor force, T_a, are computed, by imposing the force and moment equilibrium of the wall.

2.2 *Anchor wall*

Figure 1 shows also a typical layout of a steel sheet pile anchorage (top depth c, tie-rod depth b_A, toe depth H_A, location L). For a given k_h, the proposed earth pressure diagram provides the ultimate load that can be sustained by the anchor, T_{lim}, taking into account the possible rotation induced by an eccentric anchor force. Above the pivot point H_0, the soil is in active limit state and in passive limit state behind and in front of the wall, respectively. Below H_0, active and passive limit states switch sides, in view of a quite rigid response of the anchor wall. The two unknowns of the problem, H_0 and T_{lim}, are affected by the eccentricity of the anchor force over the anchor height, which is represented by the b_A/H_A ratio. Clearly, for a given k_h, T_{lim} is maximized by a balanced anchor design, corresponding to which $b_A/H_A = 2/3$.

2.3 *Plastic mechanisms and critical acceleration*

Figure 2 shows the potential failure mechanisms of the soil-wall-anchor system, related to failure of the soil, *i.e.*: (i) toe failure (TF); (ii) anchor failure (AF) and (iii) global failure (GF). Each of these corresponds to a specific value of the yield acceleration, a_y. By definition, the critical acceleration of the system is $a_c = \min(a_{y,i})$.

Toe failure occurs when the stabilizing passive earth pressure in front of the wall is completely mobilised, leading to large horizontal displacements below dredge level, which are consistent with a rotation of the wall around the top (Figure 2a). If the capacity of the anchor is reached before the full mobilization of the soil passive resistance in front of the wall, an alternative local mechanism is triggered, characterized by a rotation around a point close to the toe, and leading to large horizontal displacements near the top of the wall (Figure 2b).

Following the seminal works by Kranz (1953) and Ostermayer (1977), a global mechanism was also considered, examining the rotational limit equilibrium of a wedge of soil between the main wall and the anchor plate, sliding along a log-spiral failure surface connecting the two.

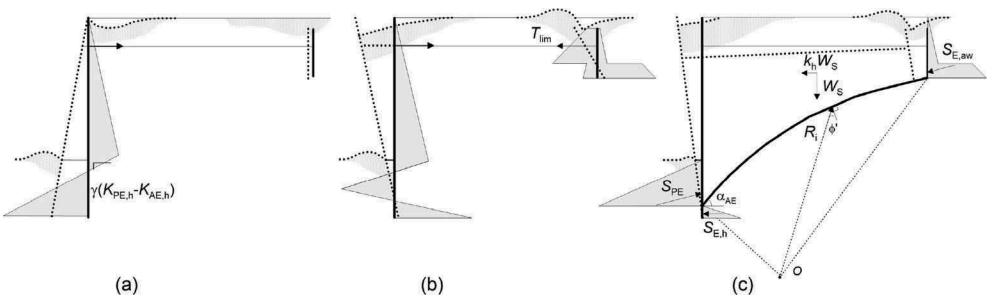

Figure 2. Potential plastic mechanisms due to the soil failure, together with the corresponding layouts of forces: (a) toe failure; (b) anchor failure; and (c) global failure.

3 DESCRIPTION OF THE NUMERICAL MODEL

3.1 *Problem layout*

Six layouts were examined in this work (see Table 1) both theoretically and numerically. Case 1, which will be discussed in detail in this paper, was assumed as a reference. The other layouts were considered to investigate the role of five dimensionless groups on the critical acceleration and hence on the overall seismic behaviour of the system. The soil properties are: $\gamma = 20$ kN/m^3, $\phi' = 35°$, $c' = 0$ kPa.

In all the layouts, an AZ 24-700 pile in S355 GP, resulting from a conventional static design procedure, was used both for the retaining wall and the sheet pile anchorage.

3.2 *Methods of analysis*

Plane-strain finite difference analyses were carried out with the code FLAC v.5 (Itasca, 2005) on a pair of ASSP walls, sufficiently distant from one another to make their seismic response independent. A first stage considered only the static equilibrium under self-weight of the base layers. After initializing the geostatic stress state in the foundation soil elements, the retaining walls and the anchors were installed, with the backfill elements activated in five successive steps, to reproduce a backfilling construction procedure. In a second stage both pseudo-static and dynamic analyses were carried out.

The soil was modelled as an elastic-perfectly plastic material, with Mohr-Coulomb failure criterion ($\phi' = 35°$, $c' = 0$ kPa) and a non-associated flow rule ($\psi = 0$). The walls were modelled as elastic beams with a stiffness $EI = 1.17 \cdot 10^5$ kNm^2/m, connected to the grid nodes with elastic-perfectly plastic interfaces characterised by a very large normal and shear stiffness ($k_n = k_s = 2 \cdot 10^7$ kN/m) and a Mohr-Coulomb failure criterion ($\delta = \phi'/3$).

Pseudo-static analyses were performed by activating a uniform body force, defined as a fraction k_h of the gravitational acceleration, in the horizontal direction. The pseudo-static coefficient was gradually increased until static equilibrium became no longer possible and a plastic mechanism appeared within the soil-wall system.

Dynamic analyses were carried out applying standard dynamic constraints along the lateral boundaries of the mesh. A set of 6 acceleration time histories, all registered on rock outcrop during real earthquakes, was applied to the bottom nodes of the grid. Table 2 summarises the corresponding ground motion parameters, *i.e.*: peak ground acceleration, *PGA*, velocity, *PGV*, and displacement, *PGD*; dominant frequency, f_d; mean frequency, f_m; Arias intensity, I_a; and duration $T_{5\text{-}95}$. Non-linear and hysteretic soil behaviour was introduced for stress paths within the yield surface through a hysteretic model available in the library of the code. More details about the numerical models can be found in Conti *et al.* (2014) and Conti & Caputo (2018).

Table 1. Problem layouts ($h = 10$ m): dimensionless geometrical data and yield accelerations.

Dimensionless groups [-]						
Case	1	2	3	4	5	6
b/h	0.10	0.10	**0.20**	0.10	0.10	0.10
D/h	0.40	0.40	0.40	0.40	0.40	**0.50**
H_A/h	0.30	0.30	0.30	0.30	**0.50**	0.30
L/h	2.10	2.10	2.10	**1.50**	2.10	2.10
b_A/H_A	0.33	**0.67**	0.67	0.33	0.35	0.33
Yield accelerations [g]						
$a_{y,TF}$	-	0.30	0.31	-	0.30	-
$a_{y,AF}$	**0.14**	-	-	0.14	-	**0.15**
$a_{y,GF}$	0.21	**0.22**	**0.22**	**0.08**	**0.20**	0.24

Table 2. Ground motion parameters of the input earthquakes.

Earthquake	PGA	PGV	PGD	f_d	f_m	I_a	$T_{5\text{-}95}$
	[g]	[m/s]	[m]	[Hz]	[Hz]	[m/s]	[s]
Kobe - Japan (1995)	0.329	0.281	0.116	0.58	3.69	1.65	11.8
Imperial Valley - USA (1979)	0.330	0.307	0.162	7.15	3.80	1.21	8.4
Hollister - Usa (1961)	0.194	0.120	0.044	0.88	2.22	0.25	14.6
Chi Chi - Taiwan (1999)	0.214	0.198	0.180	0.74	3.19	0.26	11.7
Friuli - Italy (1976)	0.324	0.222	0.042	3.78	3.28	0.76	4.2
Kocaeli - Turkey (1999)	0.337	0.609	0.502	0.78	1.45	1.31	14.7

In the discussion of dynamic results, positive accelerations are rightwards and the horizontal displacements of the walls are positive if away from the backfill.

4 RESULTS

4.1 *Pseudo-static analyses*

Figure 3(a) shows the contours of the shear strains, together with the deformed shape of the structural elements, at the onset of a plastic mechanism in the numerical model. The slip surfaces derived by the MO solution, and corresponding to the theoretical value of the critical acceleration, are also represented.

The theoretical and the numerical values of the critical acceleration are in very good agreement. A concentration of shear strains in the proximity of the sheet pile anchorage is clearly visible. Furthermore, the rotation of the anchor wall produces large horizontal displacements of the retaining wall at the anchor level and is consistent with the expected anchor failure. A local failure mechanism is also visible from the velocity field shown in Figure 3(b), which also refers to the critical conditions.

Figure 4 shows a comparison between numerical and theoretical distributions of: (a) earth pressures; (b) bending moment along the retaining wall and (c) earth pressures on the anchor wall, for $k_h = 0.0$, $k_h = 0.1$ and at $k_h = k_c$. Before the activation of the plastic mechanism in the numerical model, an arching effect occurs within the backfill, due to restricted wall movements at the anchor level. As a result, numerical horizontal stresses are higher than the assumed active value at the anchor level, and lower than active close to the excavation depth. This has two practical implications: on the one hand, the theoretical model tends to slightly overestimate the maximum bending moment in the wall, thus conferring a reasonable conservatism to the theoretical predictions; on the other hand, it always underestimates the anchor force, by a maximum amount of 20%. With k_h approaching k_c, the arching effect gradually vanishes and, for $k_h = k_c$, the earth pressure distribution above the excavation level is almost

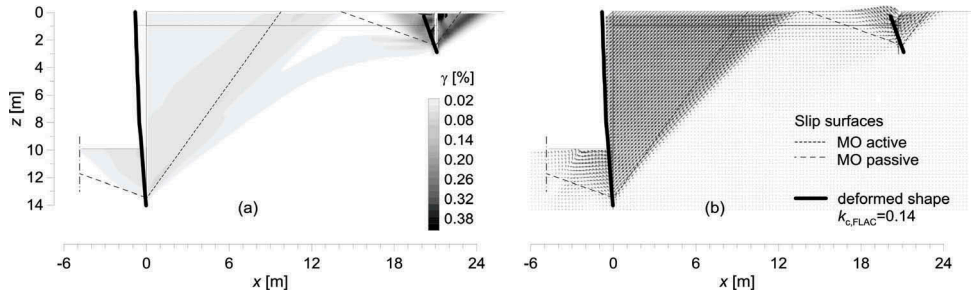

Figure 3. Pseudo-static numerical analyses: (a) contours of the shear strains and (b) field of velocities at the onset of critical conditions.

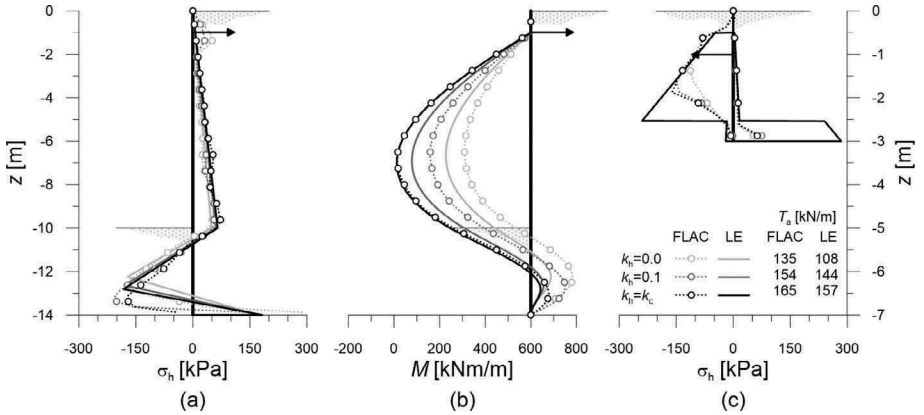

Figure 4. Numerical pseudo-static distributions of: (a) earth pressures; (b) bending moment along the wall; and (c) earth pressures on the anchor wall.

linear. In this condition, the theoretical predictions are in good agreement with the numerical results, both in terms of anchor force and maximum bending moment.

As far as the anchor wall is concerned, the proposed model allows a proper estimation of the rotation point. Some discrepancies with respect to the numerical results emerge both behind and in front of the wall, but not affecting the good prediction of the maximum allowable force, T_{lim}.

4.2 *Dynamic analyses*

The dynamic response of the system will be initially examined with respect to the Imperial Valley earthquake. Figure 5 shows the time histories of: (a, b, c) free-field and wall absolute accelerations, computed at three different depths, *i.e.,* $z = 0$ m, $z = 7$ m, and $z = 14$ m; (d) the bending moment at $z = 7.25$ m; and (e) the relative horizontal displacement of the wall. As long as the critical acceleration is not exceeded, free-field and absolute accelerations of the wall are virtually the same and no relative displacements occur. For larger values of the free-field acceleration, the wall starts to cumulate permanent displacements. In this case, the accelerations at the top and mid-height of the wall can exceed the critical value, a_c, and can be out of phase with respect to the free-field ones. However, the accelerations at the toe do not deviate significantly from the free-field ones, as the toe of the wall is only marginally involved in the failure mechanism. The relative accelerations of the wall decrease with depth, which is consistent with the ongoing rotation, driven by large horizontal displacements around the anchor level. In the light of the above, the acceleration time history at $z = 7$ m can be considered the most representative of the overall behaviour of the wall.

Figure 5(d) shows that the peaks of bending moment are always in phase with the absolute accelerations of the wall. Therefore, the maximum bending moment occurs when the inertia forces are away from the backfill, in agreement with the limit equilibrium assumption.

For all the dynamic analyses, Figure 6 shows: (a) the maximum acceleration at mid height of the wall and (b) the maximum bending moment, as a function of the maximum free-field surface acceleration. The maximum free-field accelerations are at least twice the critical acceleration of the system. As a response, the maximum accelerations of the wall are possibly larger than a_c, but indeed lower than the free-field ones and around a constant value. The same trend is even more evident in terms of maximum bending moments, which are basically independent from the intensity of the excitation. As already observed for other types of yielding retaining structures (Conti *et al.*, 2013; Conti *et al.*, 2012, 2014; Callisto 2014; Callisto & Del Brocco, 2015), and in accordance with the proposed limit equilibrium method, the dynamic response of the ASSP wall appears to be a strength-driven rather than a deformability-driven problem.

A key ingredient for the assessment of the seismic performance of ASSP walls is the maximum horizontal displacement, controlling the vertical settlements in the backfill and hence the deformations of any facilities or structures supported by the wall. Figure 6(c) shows the final displacement of the wall, due to the applied earthquakes, as function of the ratio $a_c/a_{max,ff}$ between the (theoretical) critical acceleration and the maximum free-field acceleration. As expected, the computed displacements reduce with increasing the ratio $a_c/a_{max,ff}$. Some interpolating functions proposed in the literature are also reported. That of Saygili & Rathje (2008), which derives from the application of the Newmark's sliding block procedure, would lead to non-conservative results. A similar observation concerns the interpolating function proposed by Conti & Caputo (2018), which derives from an extensive numerical study contemplating both sliding and bearing failure modes of semi-gravity cantilever walls. The authors are now conducting further investigations to predict the displacements of ASSP walls.

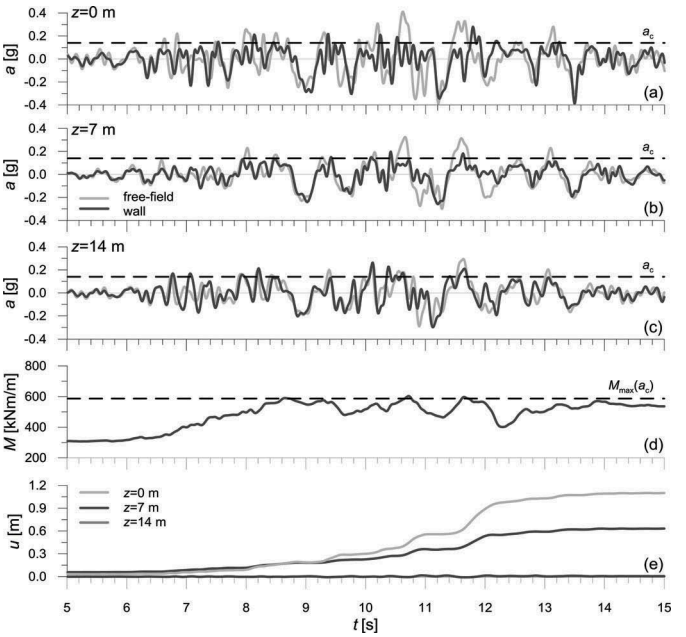

Figure 5. Time histories of: (a, b, c) horizontal free-field and wall absolute accelerations at three depths; (b) bending moment at $z = 7.25$ m and (c) horizontal displacements of the wall.

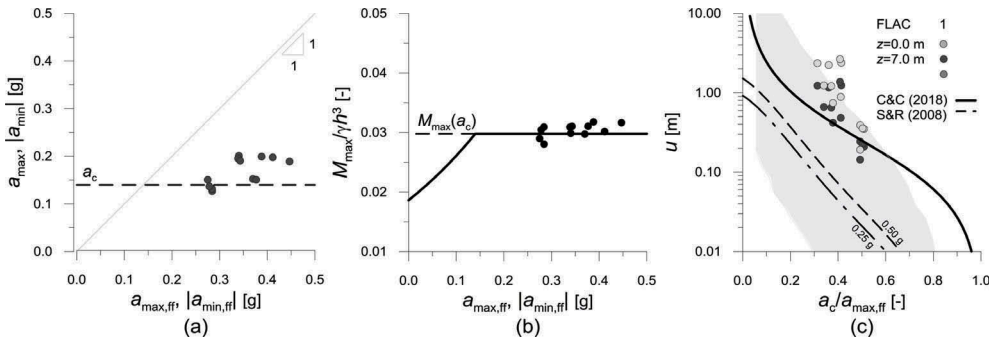

Figure 6. Numerical dynamic analyses: (a) maximum wall absolute accelerations; (b) maximum bending moments *vs* $a_{max,ff}$ and (c) final dynamic incremental displacements *vs* $a_c/a_{max,ff}$.

5 CONCLUSIONS

The emerging demand for performance-based design methodologies involves a more thorough understanding of the seismic response of ASSP walls. The actual performance of yielding ASSP walls suggests that a more rational and economical approach to the design should consider an appropriate design acceleration, related to a selected wall performance, rather than the prescribed maximum seismic acceleration. Nevertheless, the wall-soil interaction problem is more complex compared with other type of retaining structures and the conventional force-balanced approach, aiming for an extremely simplification, might result inappropriate.

The work described in this paper has addressed some of the current shortcomings preventing the adoption of simplified displacement methods for ASSP walls. Possible failure mechanisms were investigated in terms of earth pressure distributions and shape of the potential failure surfaces developing within the soil. Specific methods were proposed to calculate the critical acceleration of the system and predict the maximum internal forces in the structural elements.

They were validated through an extensive numerical study, which also highlighted the key role of the critical acceleration limiting the maximum internal forces in the structural members and controlling the magnitude of permanent displacements.

REFERENCES

Anderson, D.G., Martin, G.R., Lam, I., and Wang, J.N. 2008. Seismic analysis and design of retaining walls, buried structures, slopes, and embankments. NCHRP Rep. 611, Transportation Research Board, Washington, D.C.

Callisto L. 2014. Capacity design of embedded retaining structures. *Géotechnique* 64, No. 3, 204-214.

Callisto L., Del Brocco I. 2015. Intrinsic seismic protection of cantilevered and anchored retaining structures. *In Proceedings of the SECED Conference on Earthquake Risk and Engineering towards a Resilient World*, Cambridge, UK, 9-10, July, 2015.

Conti, R., Madabhushi, S.P.G. and Viggiani, G.M.B 2012. On the behaviour of flexible retaining walls under seismic actions. *Géotechnique*, 62(12),1081-1094.

Conti, R., Viggiani, G.M.B., Cavallo, S. 2013. A two-rigid block model for sliding gravity retaining walls. *Soil Dyn. Earth. Eng*., 55, 33-43.

Conti, R., Viggiani, G.M.B, Burali d'Arezzo, F. 2014. Some remarks on the seismic behaviour of embedded cantilevered retaining walls. *Géotechnique*, 64(1),40-50.

Conti, R. & Caputo, G. 2018. A numerical and theoretical study on the seismic behaviour of yielding cantilever walls. *Géotechnique*, DOI: 10.1680/jgeot.17.P.033

Elms D. A., and G. R. Martin 1979. "Factors Involved in the Seismic Design of Bridge Abutments." *Proceedings, Workshop on Seismic Problems Related to Bridges, Applied Technology Council*, San Diego, Calif.

Itasca, 2005. FLAC Fast Lagrangian Analysis of Continua v. 5.0. User's Manual.

Kranz, E., 1953. Ueber die Verankerung von Spundwanden. W. Ernst & Sohn, Berlin.

Lai, S., 1998. "Rigid and flexible retaining walls during Kobe earthquake", *Fourth International Conference on Case Histories in Geotechnical Engineering*, Paper No. SOA-4, St. Louis, Missouri, 1998.

Lancellotta, R. 2007. "Lower-Bound approach for seismic passive earth resistance". *Géotechnique*, Vol. 57, No. 3, pp. 319-321.

Mononobe N., Matsuo H., 1929. On the determination of earth pressure during earthquake. *In Proc. 2nd World Engineering Conference*, volume 9, pp. 177–185.

Neelakantan, G., Budhu, M. and Richards, R., Jr., 1990. "Mechanics and Performance of a Tied-Back Wall Under Seismic Loads", *Earthquake Engineering and Structural Dynamics*, Vol. 19, No. 3, 315-332

Newmark N. M., 1965. Effects of earthquakes on dams and embankments. *Géotechnique*, 15(2),139–160.

Okabe S., 1926. General theory of earth pressure. *Journal of Japanese Society of Civil Engineering*, 12(1).

Ostermayer H., 1977. "Practice in the Detail Design Application of Anchorages," *A Review of Diaphragm Walls*, Institution of Civil Engineers, London, 1977, pp. 55-61.

Richards, R., Elms, D.G. 1979. Seismic behaviour of gravity retaining walls. *J. Geotech. Eng. Div*., ASCE, 105(4),449-464.

Saygili, G., Rathje, E.M. 2008. "Empirical Predictive Models for Earthquake-Induced Sliding Displacements of Slopes". *J. Geotech. Geoenviron. Eng*., 134(6),790-803.